Hindawi
Advances in Civil Engineering
Volume 2019, Article ID 4892015, 12 pages
https://doi.org/10.1155/2019/4892015

Research Article

Evaluation of Strengths from Cement Hydration and Slag Reaction of Mortars Containing High Volume of Ground River Sand and GGBF Slag

Punnaman Norrarat,[1] Weerachart Tangchirapat ,[2] Smith Songpiriyakij,[3] and Chai Jaturapitakkul[4]

[1]*Concrete Testing Manager, Siam Research and Innovation Co., Ltd., Saraburi 18260, Thailand*
[2]*Assistant Professor, Department of Civil Engineering, Faculty of Engineering, King Mongkut's University of Technology Thonburi, Bangkok 10140, Thailand*
[3]*Associate Professor, Department of Civil and Environmental Engineering Technology, College of Industrial Technology, King Mongkut's University of Technology North Bangkok, Bangkok 10800, Thailand*
[4]*Professor, Department of Civil Engineering, Faculty of Engineering, King Mongkut's University of Technology Thonburi, Bangkok 10140, Thailand*

Correspondence should be addressed to Weerachart Tangchirapat; weerachart.tan@kmutt.ac.th

Received 15 January 2018; Accepted 27 December 2018; Published 23 January 2019

Academic Editor: Cumaraswamy Vipulanandan

This paper investigates the cement hydration, and the slag reaction contributes to the compressive strengths of mortars mixed with ground river sand (GRS) and ground-granulated blast furnace (GGBF) slag with different particle sizes. GRS (inert material) and GGBF slag (reactive material) were ground separately until the median particle sizes of 32 ± 1, 18 ± 1, and 5 ± 1 micron and used to replace Portland cement (PC) in large amount (40–60%) by weight of the binder. The results showed that, at the early age, the compressive strength obtained from the cement hydration was higher than that obtained from the slag reaction. The results of compressive strength also indicated that the GGBF slag content and particle size play important roles in the slag reaction at the later ages, whereas cement hydration is more prominent at the early ages. Although the results could be expected from the use of GGBF slag to replace PC in mortar or concrete, this study had presented the values of the compressive strength along with ages and the finenesses of GGBF slag that contributed from cement hydration and from GGBF slag reaction.

1. Introduction

Blast furnace slag (BFS) is an industrial by-product of the manufacturing of pig iron. In the production of the pig iron process, iron ore and limestone (as a flux) are burnt together by coke at 1500°C in a blast furnace. Liquid slag and liquid pig iron are products. The liquid slag has a lower density than liquid pig iron and floats on the top of the liquid pig iron. After being separated from the liquid pig iron, the liquid slag was quenched with water to form glassy granular particles called granulated blast furnace (GBF) slag. GBF slag exhibits hydraulic cementing properties when it is finely ground, and it is called ground-granulated blast furnace (GGBF) slag or slag cement [1]. GGBF slag has been used as a supplementary cementitious material (SCM) in blended cement, and annual worldwide production of GGBF slag is estimated at 250 million tons a year [2].

The benefits of GGBF slag (when used as a partial replacement in cement) include the enhancement of long-term strength and durability of concrete, cost reduction, and a reduced environmental impact [3, 4]. In addition, the heat evolution was reduced when the replacement of GGBF slag was increased [5]. GGBF slag is specified by ASTM C989 [6] in three grades (Grade 80, Grade 100, and Grade 120),

depending on the relative mortar strength. The common dosages of GGBF slag in blended cement have been varied from 6 to 95% according to BS EN 197-1 [7] and can be used in cement production according to ASTM C595 [8] and ASTM C1157 [9].

There are 3 major processes contributing to the compressive strength of mortars or concretes containing GGBF slag: the hydration of Portland cement, the GGBF slag reaction, and the packing effect of small particles. Celik [10] studied the effect of particle size distribution and fineness of Portland cement (PC) on the strength development and found that the fineness of PC is the major factor affecting the strength development of mortar, especially in the early age of cement hydration.

PC hydration and GGBF slag reaction are chemical reactions between PC, GGBF slag, and water. The main products of the hydration reaction are calcium silicate hydrate (C-S-H), calcium aluminate hydrate (C-A-H), and calcium hydroxides ($Ca(OH)_2$). $Ca(OH)_2$ released from the hydration of the calcium silicate phase in PC can react with SiO_2 and Al_2O_3 in GGBF slag to form C-S-H and C-A-H. Additionally, calcium oxide (CaO) in GGBF slag can create C-S-H from the hydration similar to PC hydration, but it is a much slower rate [11]. The slag reaction of GGBF slag is very complex, which depends on the chemical composition, mineralogical composition, glass content, and fineness of the GGBF slag [12]. The slag reaction is one of the most important properties to consider when assessing the suitability of SCM in replacing PC in concrete production [13].

Binder materials with small particles can also improve the compressive strength due to the packing effect or filler effect by physically filling the spaces without any chemical reaction [14]. Furthermore, the replacement of PC with an optimal dosage of highly refined SCM can reduce the pore structure and porosity of concrete, resulting in dramatically decreased penetration of aggressive chloride ions into the concrete [15, 16]. Many researchers [15, 17, 18] reported that ground river sand (GRS) in the form of quartz with the same particle size as PC and pozzolanic material can be used as an inert material to evaluate compressive strengths obtained from cement hydration, pozzolanic reactions, and packing effect. However, only a few reports on the reaction of GGBF slag have been presented.

Norrarat et al. [19] investigated the heat evolution pastes containing inert and reactive materials (ground river sand and GGBF slag) with different particle sizes using an isothermal conduction calorimeter. The results showed that the heat evolution obtained from the slag reaction increased with the increase of GGBF slag content in the pastes. Kocaba et al. [20] studied the methods for determination of degree of reactions of pastes containing GGBF slag using an isothermal conduction calorimeter, selective dissolution, differential scanning calorimetry, image analysis, and chemical shrinkage. Jaturapitakkul et al. [21] used GRS in the form of quartz with the same particle size as PC (median particle size of 11.5 micron) as an inert material to evaluate compressive strengths obtained from cement hydration and packing effect. However, their study did not cover the packing effect and the slag reaction of GGBF slag contributing to the compressive strength.

It is expected that the mortar containing GRS, which is in a crystalline phase, can provide a compressive strength from cement hydration. Thus, the compressive strength of mortar obtained from the slag reaction was the different value of the compressive strength of GGBF slag mortar and the compressive strength of GRS mortar, when the same cement replacement rate, same fineness of PC, GRS, and GGBF slag, same workability, and same curing age of mortars are considered.

Therefore, the aim of this paper is to evaluate the compressive strength of mortar obtained from the cement hydration and from the slag reaction when GRS and GGBF slag with different particle sizes are used to replace PC in large amounts (40 to 60%) by weight of the binder. This study based on the assumption that the packing effect value of GRS and GGBF slag is little or no in the mortar, if PC, GRS, and GGBF slag have the same particle size. These results lead to a better understanding of the factors affecting the rate of reaction of GGBF slag. The results of this study may be helpful for cement and concrete manufacturers in selecting suitable fineness of GGBF slag to replace a portion of PC. Moreover, the filler (ground river sand) with the same particle size as PC may be used as a partial replacement of PC because it is known how much the compressive strength decreased when the PC was replaced by ground river sand.

2. Materials and Methods

2.1. Materials. The materials used in this study consisted of Portland cement type I (PC) according to ASTM C150 [22], ground river sand (GRS), ground-granulated blast furnace (GGBF) slag, local river sand, and water. GGBF slag, a by-product of the production of pig iron, was obtained from the Eastern part of Thailand. Local river sand passed 1.18 mm (no. 16) mesh and retained on 150 μm (no. 100) mesh and was used as a fine aggregate. The fineness modulus and the water absorption of the fine aggregate were 2.34 and 0.72%, respectively.

River sand and GBF slag were ground separately using a ceramic ball mill to have three different median particle sizes (d_{50}) of 32 ± 1, 18 ± 1, and 5 ± 1 μm. These sizes are specified as *L* (large-sized), *M* (medium-sized), and *S* (small-sized). After grinding, the binder materials are called ground-granulated blast furnace (GGBF) slag and ground river sand (GRS).

2.2. Physical Properties of Materials. Physical properties of PC, GRS, and GGBF slag with different particle sizes are given in Table 1. PC has a median particle size (d_{50}) of 18.1 μm and has a specific gravity, and a weight of the particle retained a 45 μm (no. 325) of 3.15 and 16.6%, respectively. LGRS, MGRS, and SGRS have median particle sizes (d_{50}) of 32.2, 17.7, and 4.8 μm, respectively, while those for LGGBF, MGGBF, and SGGBF slag are 32.0, 17.8, and 4.4 μm, respectively. ASTM C989 [6] specified that the particles of GGBF slag retained on a 45 μm·mesh (no. 325) shall not be higher than 20% by weight. Table 2 shows the mineralogical compositions of GRS and GGBF slag

Table 1: Physical properties of PC, GRS, and GGBF slag.

Materials	Specific gravity	Retained on a no. 325 sieve (%)	Median particle size, d_{50} (μm)
PC	3.15	16.6	18.1
LGRS	2.62	38.3	32.2
MGRS	2.61	17.9	17.7
SGRS	2.63	1.1	4.8
LGGBF	2.92	37.6	32.0
MGGBF	2.92	12.2	17.8
SGGBF	2.92	2.4	4.4

Table 2: Mineralogical compositions of GRS and GGBF slag.

Materials	Crystalline (%)				Amorphous (%)
	Quartz	Microcline	Albite	Muscovite	
LGRS	79.5	13.6	3.8	3.1	—
MGRS	79.4	13.6	3.9	3.1	—
SGRS	79.4	13.8	3.8	3.0	—
LGGBF	0.5	—	—	—	99.5
MGGBF	0.8	—	—	—	99.2
SGGBF	0.4	—	—	—	99.6

determined by using quantitative X-ray diffraction analysis. LGRS, MGRS, and SGRS consist of 100% crystalline phases (quartz, microcline, albite, and muscovite), whereas LGGBF, MGGBF, and SGGBF slag consist of 99.5, 99.2, and 99.6% amorphous or glass content.

The particle shapes of PC, MGRS, and MGGBF slag as shown in Figure 1 were determined by a scanning electron microscope. All of them had solid angular particles with some rough surfaces. Figure 2 shows the particle size distributions of PC, GRS, and GGBF slag. It should be noted that the particle size distributions and the d_{50} of PC, MGRS, and MGGBF slag were very similar which were in the range of $18 \pm 1\,\mu$m (Figure 2(b)). This process was intended to avoid the particles packing effect when ground river sand (GRS) or GGBF slag was used to partially replace PC. The particle size distributions and the d_{50} of LGRS and LGGBF slag (Figure 2(a)) and SGRS and SGGBF slag (Figure 2(c)) were nearly the same which were in the range of 32 ± 1 and $5 \pm 1\,\mu$m, respectively.

2.3. Chemical Composition of Materials. Chemical components of PC, LGRS, and LGGBF slag, which are determined by using X-ray fluorescence analysis, are shown in Table 3. The main chemical component of the PC was CaO (65.0%), whereas the main chemical component of LGRS was SiO_2 (93.6%). The SiO_2 was in the form of quartz; thus, it was not a pozzolanic material.

Similar results of ground river sand containing approximately 91.8–92.9% SiO_2 (quartz) were reported by Tangpagasit et al. [17] and Yang et al. [23], respectively. Quartz is normally recognized as a chemically inert material [24, 25]. Thus, GRS is an inert material and cannot react with PC or GGBF slag.

LGGBF slag had the major chemical components of 35.6% CaO, 36.4% SiO_2, 14.6% Al_2O_3, and 7.1% MgO and other minor components including alkali and iron oxides. Figures 3 and 4 show the X-ray diffraction patterns of SGRS and SGGBF slag, respectively. The results also showed that SGRS consisted mostly in a crystalline peak, whereas SGGBF slag was in a noncrystalline or amorphous peak.

2.4. Mortars. To evaluate the compressive strength contributing from cement hydration, slag reaction, and packing effect, three types of mortars, Portland cement mortar made with Portland cement type I (PC mortar), inert material mortar (GRS mortar), and GGBF slag mortar, were prepared and investigated in this study. The PC mortar contained only PC as a binder. GRS or GGBF slag was used separately as a binder material to replace PC at rates of 0, 40, 50, and 60% of total binder (PC or PC + GRS or PC + GGBF slag) by weight. Mortar mixture had a ratio of binder to fine aggregate as 1 to 2.75 by weight. The flows of all fresh mortars were controlled in the range of $110 \pm 5\%$ by adjusting the mixing water. The method for measuring the flow of mortar followed ASTM C230 [26].

Mortar cube specimens ($50 \times 50 \times 50$ mm) were cast for testing compressive strength and the specimens were covered with a plastic sheet to prevent the evaporation of water after finishing casting. After casting for 24 h, the mortars were demolded and then cured in saturated lime water at $23 \pm 2^{\circ}$C until the age of testing.

Table 4 shows the mix proportions, water-to-binder ratio (W/B), and the flow of PC mortar, GRS mortar, and GGBF slag mortar. It was found that the PC mortar had the flow 107% with W/B ratio of 0.54. The GRS mortars produced flows ranging from 105–115% with W/B ratios from 0.53 to 0.55, whereas GGBF slag mortars produced flows ranging from 106–115% with W/B ratios from 0.53 to 0.55. Since all of the binders (PC, GRS, and GGBF slag) had almost the same fineness (Table 1), the same shape of particles (Figure 1), and the same particle size distributions (Figure 2), the W/B ratios of all mortars were almost the same and in the ranges of 0.53–0.55. This suggests that the difference in the compressive strengths of GRS and GGBF slag mortars due to the different W/B ratios was assumed to be small and could be neglected. This means that the results of the influence of the slag reaction and the replacement rate of the GRS and GGBF slag seemed to be the major factors affecting the compressive strength of mortars.

The compressive strengths of the mortars were determined according to ASTM C109 [27] at ages of 3, 7, 28, 90, and 180 days. The load was applied to the mortar specimen with the force control and the rate in the range of

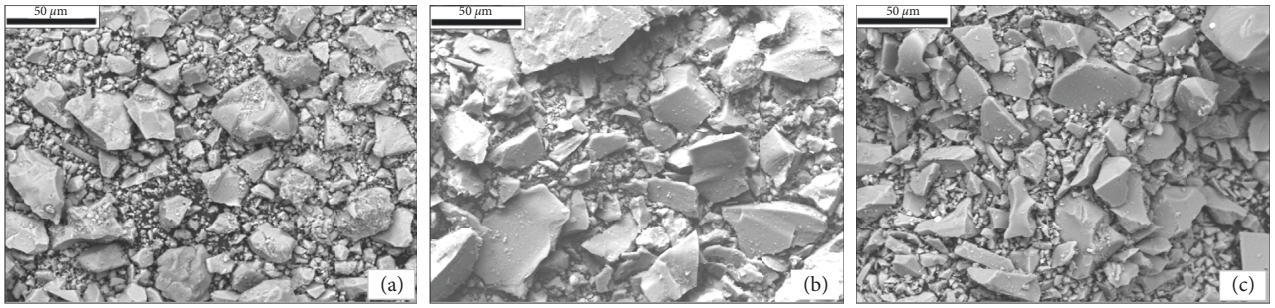

Figure 1: Particle shapes by scanning electron microscopy images: (a) PC; (b) MGRS; (c) MGGBF slag.

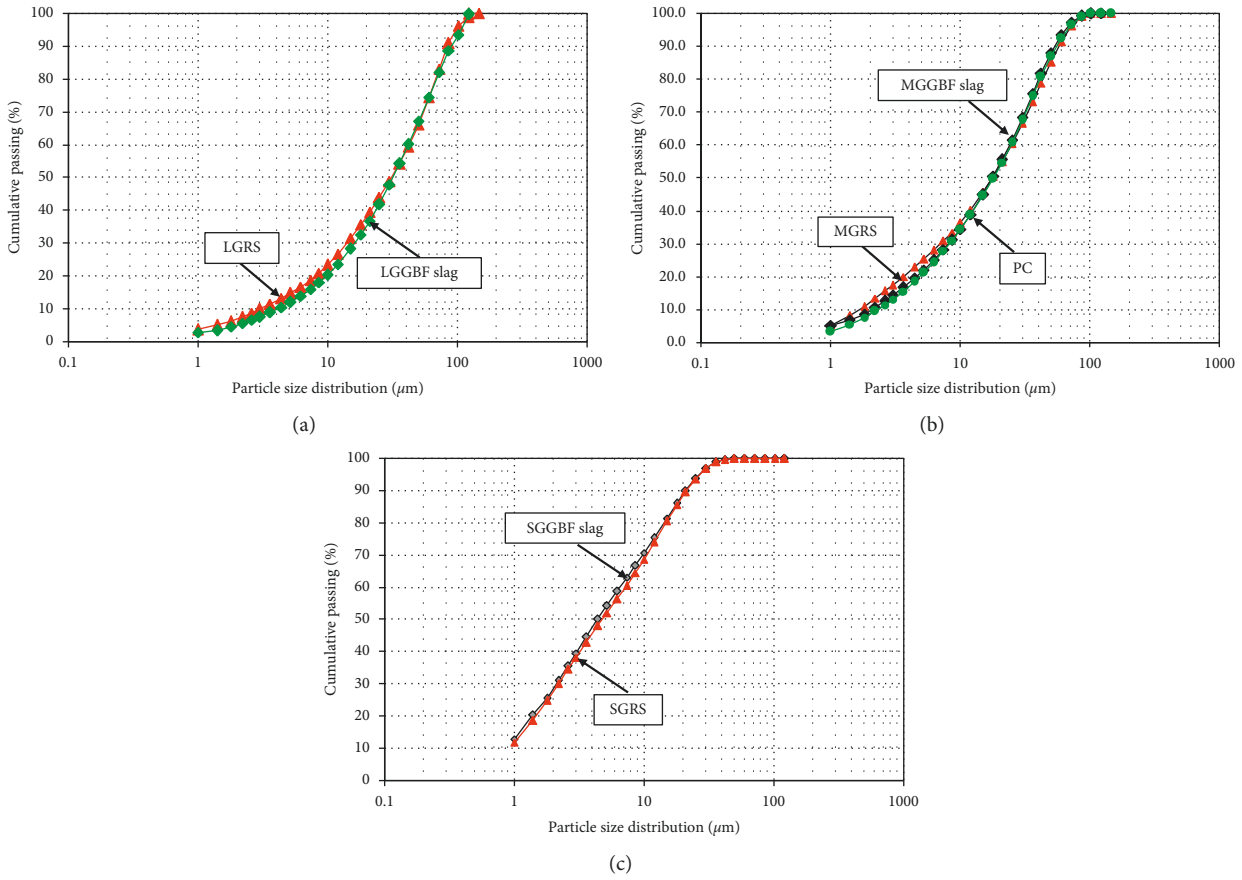

Figure 2: Particle size distributions of PC, GRS, and GGBF slag: (a) particle size distributions of LGRS and LGGBF; (b) particle size distributions of MGRS, MGGBF, and PC; (c) particle size distributions of SGRS and SGGBF.

Table 3: Chemical compositions of PC, LGRS, and LGGBF slag.

Materials	Chemical compositions (%)								
	SiO_2	Al_2O_3	Fe_2O_3	CaO	SO_3	Na_2O	K_2O	MgO	LOI
PC	19.5	5.3	3.2	65.0	2.7	0.1	0.4	0.8	2.4
LGRS	93.6	4.3	0.3	0.1	0.0	0.4	0.3	0.1	0.4
LGGBF slag	36.4	14.6	1.5	35.6	1.9	0.2	1.3	7.1	0.6

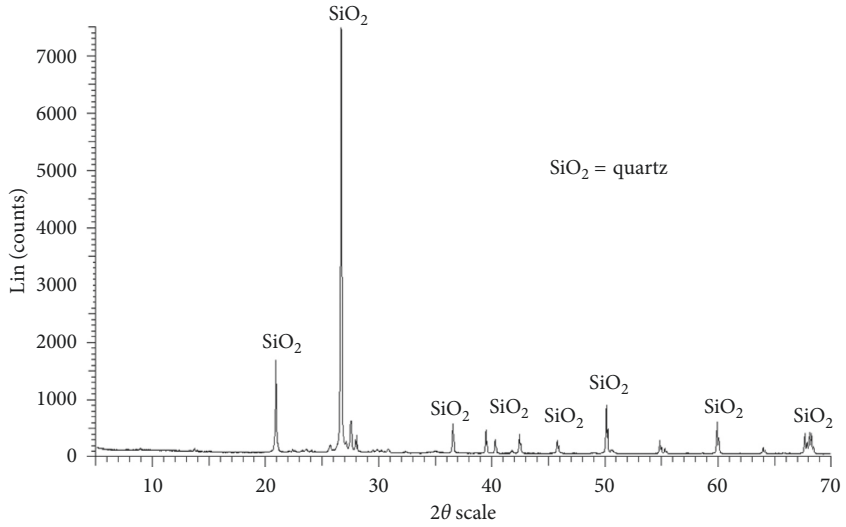

Figure 3: X-ray diffraction pattern of a SGRS with a characteristic crystalline peak.

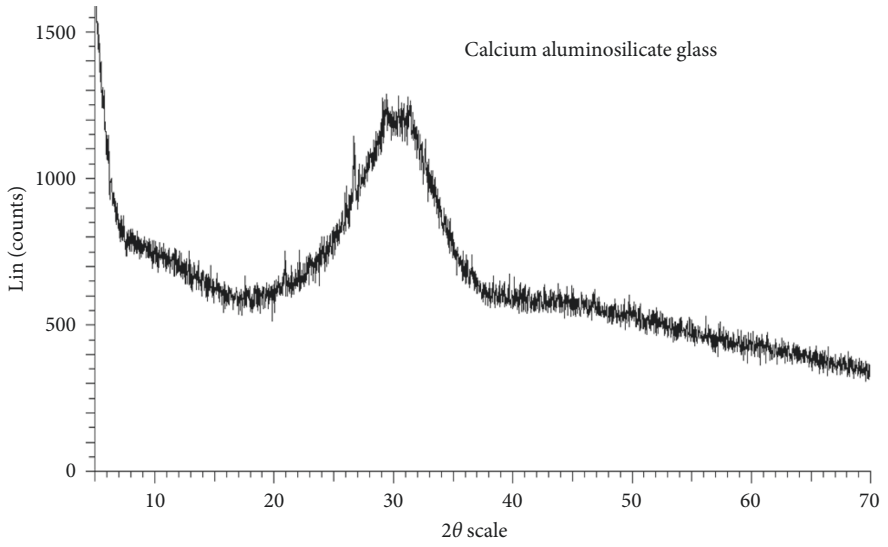

Figure 4: X-ray diffraction pattern of a SGGBF slag with a characteristic amorphous peak.

900 to 1800 N/sec. For each testing age, five mortars specimens were used as an average value, with the acceptable range of the tested results being within 8.7%.

3. Results and Discussion

3.1. Slag Activity Index. According to ASTM C989 [6], GGBF slag has 3 grades that depend on the mortar strength, i.e., grade 80, 100, and 120. The slag activity index (SAI) of mortar using GGBF slag to replace PC at a rate of 50% by weight of the binder will not be less than 75% of the strength of the PC mortar at 28 days for grade 80. Grade 100 must obtain an SAI of more than 70% at 7 days and 90% at 28 days. For grade 120, SAI shall be less than 90% at 7 days and 110% at 28 days.

From the results of SAI or the percentage of compressive strength of mortars as compared to PC mortar, the mortars containing LGGBF slag with the median particle size of 32.0 μm had SAI less than 70% at 28 days (62.2%). SAI of the MGGBF ($d_{50} = 17.8\,\mu$m) mortars at 7 and 28 days was 53.5 and 78.3%, respectively, and was classified as grade 80 according to ASTM C989 [6]. SAI of the SGGBF ($d_{50} = 4.4\,\mu$m) mortars at 7 and 28 days was 73.6 and 105.4%, respectively. SGGBF slag can be categorized as grade 100 according to ASTM C989 [6].

The SAI or the compressive strength of GGBF slag mortars increasing with age could be observed clearly at 180 days. The results of mortars at 90 and 180 days indicated that there was continuous and significant improvement in the SAI beyond the age of 28 days. For example, the SAI of mortars MGGBF50 and SGGBF50 at the age of 28 days was 78.3 and 105.4% of the control mortar, respectively. At the ages of 90 and 180 days, the SAI increased to 95.1 and 103.1% and 122.7 and 123.5% of the PC mortar, respectively. The increases in SAI from 28 days to 90 and 180 days were 16.6 and 24.6% and 17.0 and 18.1%, respectively, which suggests

Table 4: Mix proportions of mortars by weight.

Mixture	PC	GRS	GGBF Slag	Fine aggregate	W/B	Flow (%)
PC	1.0	—	—	2.75	0.54	107
LGRS40	0.6	0.4	—	2.75	0.53	106
LGRS50	0.5	0.5	—	2.75	0.54	105
LGRS60	0.4	0.6	—	2.75	0.54	105
MGRS40	0.6	0.4	—	2.75	0.54	111
MGRS50	0.5	0.5	—	2.75	0.55	105
MGRS60	0.4	0.6	—	2.75	0.54	113
SGRS40	0.6	0.4	—	2.75	0.53	106
SGRS50	0.5	0.5	—	2.75	0.54	115
SGRS60	0.4	0.6	—	2.75	0.55	111
LGGBF40	0.6	—	0.4	2.75	0.53	106
LGGBF50	0.5	—	0.5	2.75	0.53	112
LGGBF60	0.4	—	0.6	2.75	0.55	112
MGGBF40	0.6	—	0.4	2.75	0.54	114
MGGBF50	0.5	—	0.5	2.75	0.54	113
MGGBF60	0.4	—	0.6	2.75	0.53	114
SGGBF40	0.6	—	0.4	2.75	0.53	106
SGGBF50	0.5	—	0.5	2.75	0.53	115
SGGBF60	0.4	—	0.6	2.75	0.53	115

that the particle size, replacement, and curing age of GGBF slag significantly influenced the SAI.

3.2. Effect of GRS Replacement on the Compressive Strength. Table 5 shows the compressive strength of the PC mortar and mortars containing GRS with different particle sizes at the cement replacement rates of 40, 50, and 60% by weight of the binder. It was observed that the 3, 7, and 28 days compressive strengths of the PC mortar were 30, 41.3, and 52.1 MPa, respectively, and revealed that the compressive strengths of the PC mortar increased very quickly up to 28 days (increasing from 30 MPa at 3 days to 52.1 MPa at 28 days). After 28 days, the compressive strengths increased slightly, and the compressive strengths of the PC mortar at 90 and 180 days were 54.7 and 55.0 MPa, respectively.

For mortars containing GRS, the compressive strengths of the LGRS, MGRS, and SGRS mortars decreased with the increasing GRS replacement. The mortars containing GRS contents at 50 and 60% showed lower compressive strengths than the mortar with GRS 40% at the same age because GRS is an inert material (SiO_2 of GRS in the form of quartz) and cannot react with cement and water to create the strength from the chemical reaction [24]. Thus, the PC content of the GRS mortar was decreased as the high replacement of GRS (40 to 60% in the binder) increased, resulting in a reduction of calcium silicate hydrated from the hydration of Portland cement.

Figure 5 shows the percentage of compressive strength of mortars containing GRS with different particle sizes as compared to PC mortar. This finding suggests that the mortars mixed with all particle sizes of GRS provided much lower compressive strength than that of the control mortar at all testing ages. The results were also indicating that the percentage of compressive strengths of MGRS and LGRS mortars were slightly lower than that of SGRS mortar at the same replacement rate of PC and same testing age. This could be attributed to the small particle size of SGRS producing higher particle packing and creating a more homogeneous paste and denser paste [28].

Table 5: Compressive strengths of mortars containing ground river sand (GRS).

Mixtures	Flow (%)	Compressive strength (MPa)				
		3 days	7 days	28 days	90 days	180 days
PC	107	30.0	41.3	52.1	54.7	55.0
LGRS40	106	10.7	14.8	18.7	19.6	19.9
LGRS50	105	9.1	12.5	15.7	16.7	17.0
LGRS60	105	6.6	9.0	11.8	12.6	13.0
MGRS40	111	11.5	16.0	20.2	21.2	21.8
MGRS50	105	10.7	14.7	17.9	19.3	19.8
MGRS60	113	7.2	9.7	12.0	12.7	13.2
SGRS40	106	11.7	17.0	21.1	22.4	22.8
SGRS50	115	11.0	15.4	19.5	20.7	20.9
SGRS60	111	8.2	11.2	14.1	15.0	15.4

3.3. Evaluation of Compressive Strength of GRS Mortars due to Cement Hydration. Because the GRS is an inert material and PC and GRS have almost the same particle size distributions (Figure 2(b)), the compressive strengths of MGRS40, MGRS50, and MGRS60 mortars were only obtained from the cement hydration, and no packing effect due to GRS particles was involved as shown in Table 5.

At early ages, the strength developments of the MGRS mortars obtained from the cement hydration were much lower than that of PC mortar. At 7 days, MGRS40, MGRS50, and MGRS60 mortars had the compressive strengths obtained from the cement hydration of 16.0, 14.7, and 9.7 MPa, or 38.7, 35.6, and 23.5% of the PC mortar, respectively.

At later ages, the strength developments of the GRS mortars obtained from cement hydration were still much lower than that of PC mortar. For instance, the compressive strengths of mortars MGRS40, MGRS50, and MGRS60 at

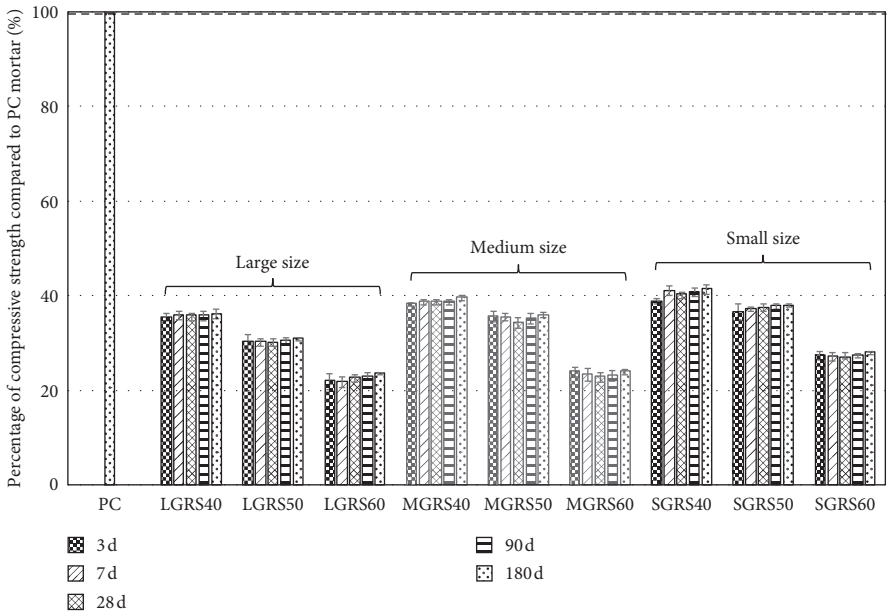

Figure 5: Percentage of compressive strength of mortars containing GRS with different particle sizes.

180 days were 21.8, 19.8, and 13.2 MPa or 39.6, 36.0, and 24.0% of the PC mortar, respectively, suggesting that the age of GRS mortar slightly affected the strength development. This is because GRS is an inert material in the form of quartz, as shown in Figure 3, and is a 100% crystalline phase such as quartz, microcline, albite, and muscovite, as determined by XRD quantitative. Thus, GRS cannot contribute the compressive strength to the mortar by the chemical reaction, and the results were conformed to those obtained by Tangpagasit et al. [17] and Kiattikomol et al. [24].

Figure 6 shows the relationship between the percentage of compressive strength of GRS mortar due to cement hydration and ages. The average percentage of compressive strengths from cement hydration at the ages of 7, 28, 90, and 180 days was 39.0, 35.3, and 23.4% for the MGRS40, MGRS50, and MGRS60 mortars, respectively. According to Figure 6, the percentage compressive strengths of the mortars (MGRS40, MGRS50, and MGRS60) were almost constant from 7 days to 180 days.

Similar results for GRS mortars were reported by Jaturapitakkul et al. [18] who found that the percentages of compressive strengths of mortar with W/B ratio of 0.49 obtained from the hydration of Portland cement were 89.0, 80.6, 73.5, and 58.0% of the PC mortar, respectively, with the replacements of GRS of 10, 20, 30, and 40%, respectively. Moreover, Sata et al. [29] studied the mortars with a W/B ratio of 0.58 containing GRS (10 to 40% replacement rates of cement) and found that the percentages of compressive strengths of GRS mortar obtained from the cement hydration were 93.1, 83.4, 73.4, and 58.2% of the PC mortar, respectively.

It should be noted that the difference in compressive strength of GRS 40 mortar obtained from this study compared with those of Jaturapitakkul et al. [18] and Sata et al. [29] could be explained as having two reasons: (1) the different the fineness of GRS and Portland cement, the higher the fineness and the greater the compressive strength due to the hydration reaction, and (2) with the different W/B ratios of mortar, the compressive strength of mortar due to the hydration reaction increases with W/B ratio.

3.4. Evaluation of Compressive Strength of GGBF Slag Mortars due to Slag Reaction. The results of the compressive strength of GGBF slag mortars with different particle sizes are shown in Table 6. Figure 7 shows the percentage of compressive strength of GGBF mortars and the replacement of PC by the GGBF slag with different particle sizes (as compared to PC mortar). The compressive strength development of GGBF slag mortars increased with the curing age similarly to the PC mortar. It was found that the mortars mixed with smaller size of GGBF slag produce a higher compressive strength than the larger size at all testing ages. Additionally, the compressive strengths of GGBF mortars were somewhat decreased as the Portland cement replacement level increased.

At an early age of 3 to 7 days, the compressive strengths of LGGBF (d_{50} of 32.0 μm), MGGBF (d_{50} of 17.8 μm), and SGGBF (d_{50} of 4.4 μm) mortars were lower than that of the PC mortar because the cement in the mortar mixture was replaced with high amount of GGBF slag (40 to 60% replacement of PC). In addition, the compressive strengths of mortars containing GGBF slag decreased with the increased of GGBF slag replacement. The decreasing of the compressive strength with the increasing of GGBF slag is due to the lower quantity of Portland cement, such that the compressive strength obtained from the slag reaction of the GGBF slag is not high enough to compensate for the reduction in compressive strength generated by Portland cement hydration process. For instance, the 7 days compressive strengths of mortars (LGGBF50, MGGBF50, and

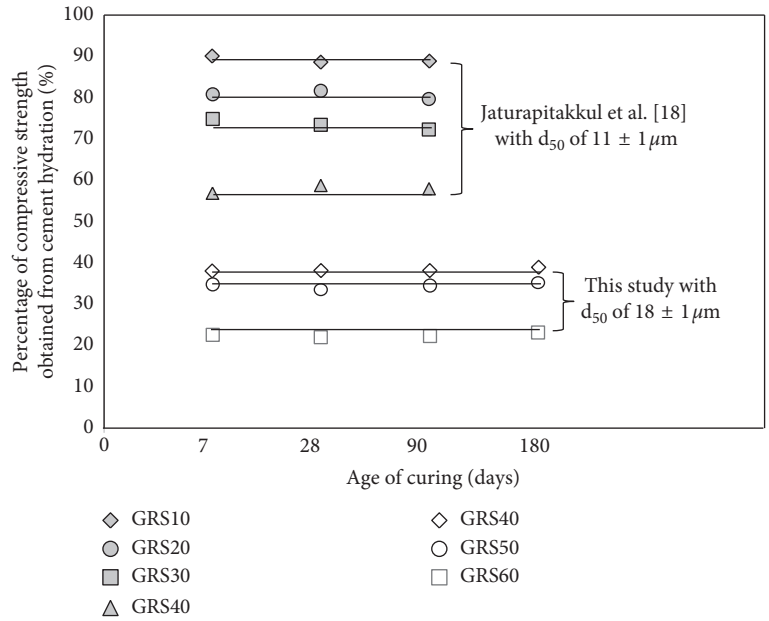

Figure 6: Relationship between percentage of compressive strength of GRS mortar and age of curing.

Table 6: Compressive strengths of mortars containing GGBF slag.

Mixtures	Flow (%)	Compressive strength (MPa)				
		3 days	7 days	28 days	90 days	180 days
PC	107	30.0	41.3	52.1	54.7	55.0
LGGBF40	106	12.6	19.0	33.4	39.4	45.0
LGGBF50	112	10.7	18.0	32.4	38.4	44.4
LGGBF60	112	8.6	12.4	28.0	36.5	42.0
MGGBF40	114	15.0	24.1	42.0	53.5	57.6
MGGBF50	113	13.2	22.1	40.8	52.0	56.7
MGGBF60	114	9.2	17.6	37.4	48.7	55.4
SGGBF40	106	17.8	31.6	55.5	68.5	69.5
SGGBF50	115	17.0	30.4	54.9	67.1	67.9
SGGBF60	115	14.1	29.2	52.0	64.4	69.3

SGGBF50) were 18.0, 22.1, and 30.4 MPa, or 43.6, 53.5, and 73.6% of the PC mortar, respectively.

The low compressive strength of the mortar containing GGBF slag was expected at early ages, and this result is consistent with the results of Douglas et al. [30]. This is because the slag reaction was slower than the hydration reaction of Portland cement at early ages [31, 32].

At the later ages of 90 and 180 days, the compressive strengths of LGGBF50, MGGBF50, and SGGBF50 mortars increased to 38.4, 52.0, and 67.1 and 44.4, 56.7, and 67.9 MPa or 70, 95, and 123 and 81, 103, and 124% of the PC mortar, respectively. The compressive strengths of GGBF slag mortars at later ages developed significantly becoming higher than that at early ages because the hydration of PC provided an alkali that activated the reaction of GGBF slag [1]. Moreover, the higher compressive strength at the later ages (after 90 days) of mortar containing GGBF slag as compared with PC mortar could be also attributed to the pozzolanic reaction between $Ca(OH)_2$ released from the Portland cement hydration process and SiO_2 and Al_2O_3 in GGBF slag to form C-S-H and C-A-H. In addition, CaO in GGBF slag can create C-S-H from the hydration reaction similar to PC, resulting in an increase in the compressive strength.

The mortars containing MGGBF and SGGBF slag contents at 40, 50, and 60% showed higher compressive strengths than that of PC mortar at the later ages (180 days) because the slag reaction of GGBF slag contributed to the development of strength [31]. The compressive strength of mortar containing GGBF slag decreased with the increased GGBF slag replacement at all testing ages, consistent with Güneyisi and Gesoğlu [32] who reported that the compressive strength of concrete-containing GGBF slag decreased with the increased GGBF slag replacement from 50 to 80%. In addition, Elahi et al. [33] found that concretes with a W/B ratio of 0.30 containing GGBF slag at 50 and 70% in a binder had the compressive strengths at 28 and 90 days of 98.6 and 74.3% and 96.8 and 77.9% of the concrete without GGBF slag, respectively.

3.5. Evaluation of the Compressive Strength of GGBF Slag Mortars Obtained from Slag Reaction. The compressive strengths of mortars containing 40, 50, and 60% GGBF slag obtained from the slag reaction are shown in Table 7. The compressive strength of mortar due to the packing effect of the small particles has to be considered and taken out from the total compressive strength. To determine the compressive strength obtained from the slag reaction, GRS and GGBF slag mortars were used to calculate. Thus, the results of the compressive strength of mortar obtained from slag reaction were the differences between the compressive strength of GGBF slag mortar and the compressive strength of GRS mortar at the same replacement rate, same fineness of GGBF slag and GRS, same workability, and same curing age of the mortars.

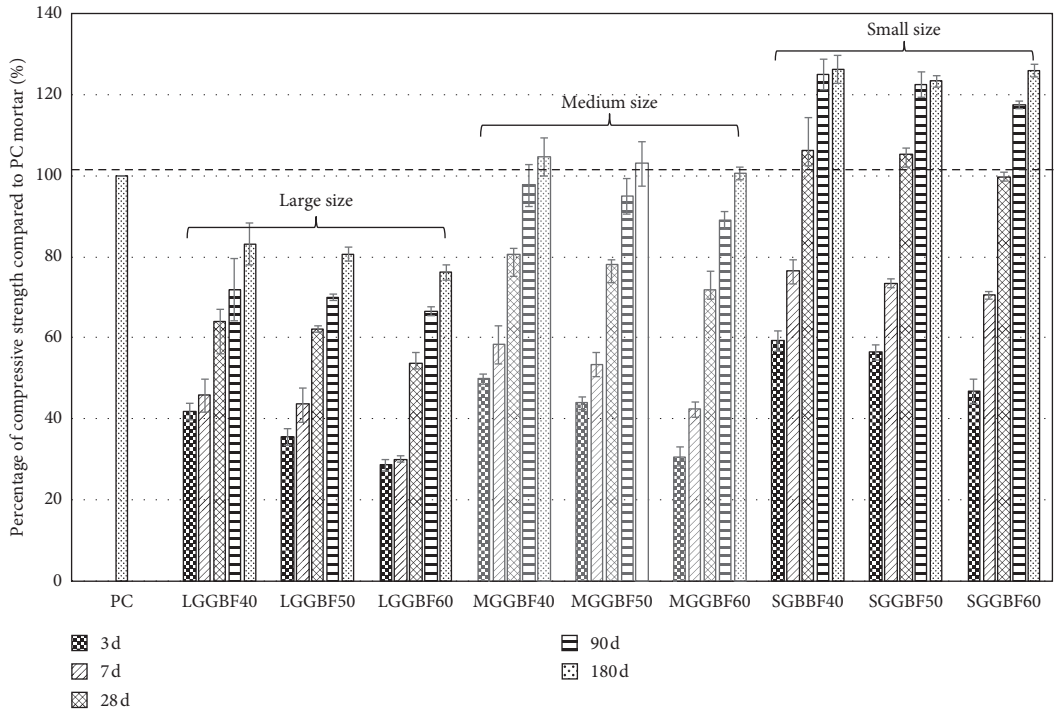

Figure 7: Percentage of compressive strength of GGBF mortar and the replacement of PC by the GGBF slag with different particle sizes.

Table 7: Compressive strengths of GGBF slag mortars obtained from the slag reaction.

Mixtures	Compared mortar	Compressive strength obtained from slag reaction (MPa)				
		3 days	7 days	28 days	90 days	180 days
LGGBF40	LGGBF40-LGRS40	1.9	4.2	14.7	19.8	25.1
LGGBF50	LGGBF50-LGRS50	1.6	5.5	16.7	21.7	27.4
LGGBF60	LGGBF60-LGRS60	2.0	3.4	16.2	23.9	29.0
MGGBF40	MGGBF40-MGRS40	3.5	8.1	21.8	32.3	35.8
MGGBF50	MGGBF50-MGRS50	2.5	7.4	22.9	32.7	36.9
MGGBF60	MGGBF60-MGRS60	2.0	7.9	25.4	36.0	42.2
SGGBF40	SGGBF40-SGRS40	6.1	14.6	34.4	46.1	46.7
SGGBF50	SGGBF50-SGRS50	6.0	15.0	35.4	46.4	47.0
SGGBF60	SGGBF60-SGRS60	5.9	18.0	37.9	49.4	53.9

For instance, the 7 days compressive strength of mortar SGGBF60 obtained from the slag reaction can be calculated as the 7 days compressive strength of mortar SGGBF60 (29.2 MPa) in Table 6 subtracting the 7 days compressive strength of mortar SGRS60 (11.2 MPa) in Table 5, which is equal to 18.0 MPa in Table 7. Figure 8 illustrates the relationships between compressive strength of GGBF slag mortar and median particle size of GGBF slag at 40 to 60% replacement of PC (compared to PC mortar) obtained from slag reaction at a specified curing age.

At the early age of 3 days, the compressive strengths obtained from the slag reaction of the LGGBF, MGGBF, and SGGBF mortars were lower than that obtained from the cement hydration. For example, the compressive strengths obtained from slag reaction of LGGBF50, MGBF50, and SGGBF50 mortars at 3 days were 1.6, 2.5, and 6.0 MPa or 5, 8, and 20% of the PC mortar, respectively, whereas those of LGRS50, MGRS50, and SGRS50 mortars were 9.1, 10.7, and 11.0 MPa or 30, 36, and 37% of the PC mortar, respectively. This is because the slag reaction was slower than the hydration of PC at the early ages [34]. In addition, Douglas et al. [30] and Bougara et al. [13] concluded that the total heat of GGBF slag during the first 24 hours is less than that of PC and the slow heat release is associated with the low early strength of GGBF slag.

At the age of 7 days, the compressive strength of the SGGBF60 mortar obtained from the slag reaction was higher than that of the SGRS60 mortar obtained from cement hydration. At the age of 28 days, the compressive strengths due to the slag reaction of MGGBF ($d_{50} = 17.8\,\mu$m) and SGGBF ($d_{50} = 4.4\,\mu$m) mortars ranged from 21.8 to 25.4 MPa and 34.4 to 37.9 MPa or 41.8 to 48.8% and 66.0 to 72.7% of the PC mortar, respectively, whereas those of MGRS ($d_{50} = 17.7\,\mu$m) and SGRS ($d_{50} = 4.8\,\mu$m) mortars ranged from 12.0 to 20.2 MPa and 14.1 to 21.1 MPa or 23.0 to 38.8% and 27.1 to 40.5% of the PC mortar, respectively. The results

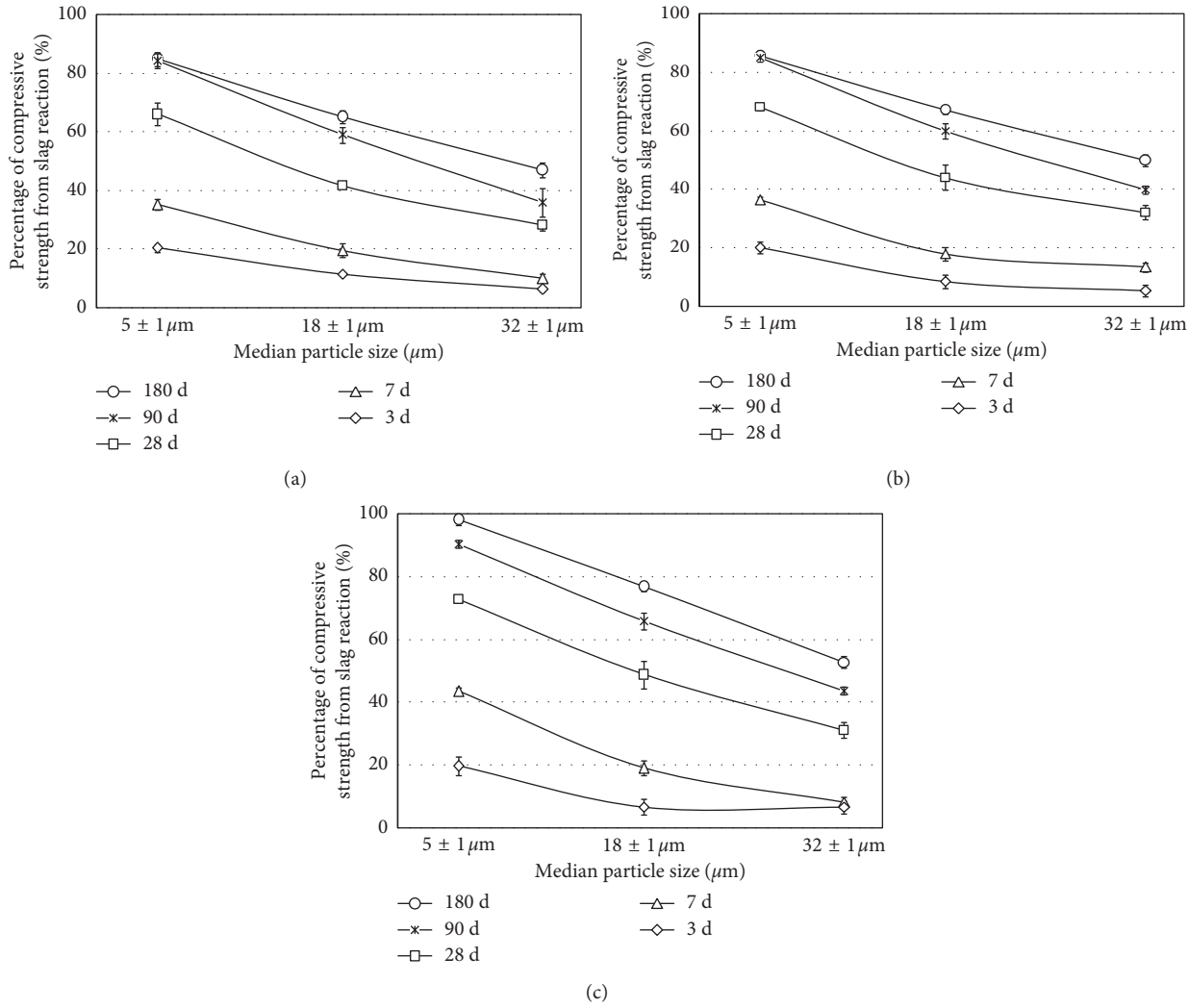

Figure 8: Relationship between percentage of compressive strength of GGBF slag mortar with different sizes (compared to PC mortar) obtained from slag reaction and age of curing: (a) 40% replacement of cement; (b) 50% replacement of cement; (c) 60% replacement of cement.

suggest that the compressive strengths at 28 days of MGGBF and SGGBF mortars obtained from the slag reaction were higher than those of the MGRS and SGRS mortars obtained from cement hydration at the same replacement level. However, the strength of LGGBF ($d_{50} = 32.0\,\mu$m) mortar obtained from the slag reaction was still lower than that of LGRS mortar obtained from cement hydration.

At the later ages of 90 and 180 days, the compressive strength of the GGBF mortars (LGGBF, MGGBF, and SGGBF) obtained from the slag reaction was still higher than that obtained from the cement hydration. For instance, the 180 days compressive strengths of mortars LGGBF60, MGGBF60, and SGGBF60 mortars were 29.0, 42.2, and 53.9 MPa, respectively, whereas those from the cement hydration of LGRS60, MGRS60, and SGRS60 mortars were 13.0, 13.2, and 15.4 MPa, respectively.

This finding suggests that the compressive strength due to the slag reaction increases with the decrease of particle size and cement replacement by GGBF slag, which can be observed clearly at the later age of 180 days. Mortar SGGBF60 had the highest compressive strength contributed from the slag reaction which was 18.0 and 53.9 MPa or 43.6 and 98.0% of the PC mortar, at 7 and 180 days, respectively. Moreover, the compressive strength of mortar obtained from the slag reaction was higher than the compressive strength of mortar obtained from the cement hydration at the later ages.

It should be noted that the GGBF slag mortar with the highest compressive strength did not necessarily have the highest strength from the slag reaction. For instance, the 180 days compressive strengths of the mortars MGGBF40 and MGGBF60 were 57.6 and 55.4 MPa, while their compressive strengths obtained from the slag reaction were 35.8 and 42.2 MPa, respectively. This suggests that the compressive strength obtained from the slag reaction depends significantly on the dosage of cement replacement and particle size of GGBF slag. In addition, a higher replacement of GGBF slag gave a higher compressive strength obtained from the slag reaction.

The improvement in the compressive strength of mortar containing GGBF slag can be explained that the GGBF slag in blended cement is comparable to the C_2S in Portland cement [35]. At early ages, the slag reaction is small or much slower than the cement hydration. Slag reaction required calcium hydroxide and an alkali from the hydration of PC to increase the reaction rate, resulting in a higher compressive strength at later ages [36]. Furthermore, at later ages, the GGBF slag produced a cementitious material that improved pore filling [37], created a denser microstructure, and enhanced the compressive strength obtained from the slag reaction when the GGBF slag replacement was increased.

4. Conclusions

The findings were summarized as follows:

(1) The optimum replacement of Portland cement type I by GGBF slag with the median particle size (d_{50}) of 17.8 μm was 60% by weight of the binder since the GGBF60 mortar gave the compressive strength as high as the PC mortar at 180 days.

(2) Compressive strengths obtained from the cement hydration of mortars containing ground river sand (GRS) at 40, 50, and 60% by weight of the binder decreased with the increased degree of GRS replacement and were 39.0, 35.3, and 23.4% of the strength of Portland cement mortar, respectively.

(3) At the early ages and the replacement of GGBF slag of 40 to 60% by weight of binder, the compressive strengths of mortars obtained from cement hydration were higher than that obtained from the slag reaction. At the later ages (28 days or more), however, the compressive strengths of mortars obtained from the slag reaction were higher than that due to cement hydration.

(4) At the early age of 3 days, mortars containing GGBF slag with the median particle sizes (d_{50}) of 32.2, 17.8, and 4.4 μm used to replace Portland cement type I at rates of 40–60% by weight of binder had the small values of compressive strengths obtained from the slag reaction and in the ranges of 1.6 to 6.1 MPa. However, at the age of 180 days, the compressive strengths obtained from the slag reaction were 25.1 to 53.9 MPa, depending on the replacement of GGBF slag.

(5) The slag reaction of GGBF slag increased with the increasing GGBF slag content in the binder and the curing age of the mortar. The result also indicated that the slag reaction of GGBF slag was small at the early ages (3 to 7 days) and increased significantly at the later ages (28 days and beyond).

Data Availability

The data used to support the findings of this study are available from the corresponding author upon request.

Disclosure

Some parts of this work were presented at the 5th International Conference of Asian Concrete Federation (ACF), 2012.

Conflicts of Interest

The authors declare that there are no conflicts of interest in this paper.

Acknowledgments

The authors gratefully acknowledge the financial supports from the Office of the Higher Education Commission, Thailand, under National Research University (NRU) and Department of Civil Engineering (CE-KMUTT 6204), King Mongkut's University of Technology Thonburi. Thanks are due to the Siam Research and Innovation Co., Ltd. for providing facilities and equipment for this study.

References

[1] ACI Committee 233R, *Slag Cement in Concrete and Mortar*, American Concrete Institute, Farmington Hills, MI, USA, 2012.

[2] O. Boukendakdji, E.-H. Kadri, and S. Kenai, "Effects of granulated blast furnace slag and superplasticizer type on the fresh properties and compressive strength of self-compacting concrete," *Cement and Concrete Composites*, vol. 34, no. 4, pp. 583–590, 2012.

[3] P. K. Metha, "Reducing the environmental impact of concrete," *Concrete International*, vol. 23, no. 10, pp. 61–66, 2003.

[4] H. A. Abola, C. K. King' Ondu, K. N. Njan, and A. L. Mrema, "Measurement of pozzolanic activity index of scoria, pumice, and rice hush ash as potential supplementary cementitious materials for Portland cement," *Advances in Civil Engineering*, vol. 2017, Article ID 6952645, 13 pages, 2017.

[5] F. Han, Z. Zhang, D. Wang, and P. Yan, "Hydration kinetics of composite binder containing slag at different temperatures," *Journal of Thermal Analysis and Calorimetry*, vol. 121, no. 2, pp. 815–827, 2015.

[6] ASTM C989, *Standard Specification for Slag Cement for Use in Concrete and Mortars*, American Society for Testing and Materials, West Conshohocken, PA, USA, 2014.

[7] BS EN 197-11, *Cement: Part 1, Composition, Specifications, and Conformity Criteria for Common Cement*, British Standards Institution, UK, 2011.

[8] ASTM C595, *Standard Specification for Blended Hydraulic Cements*, American Society for Testing and Materials, West Conshohocken, PA, USA, 2014.

[9] ASTM C1157, *Standard Performance Specification for Hydraulic Cement*, American Society for Testing and Materials, West Conshohocken, PA, USA, 2014.

[10] I. B. Celik, "The effects of particle size distribution and surface area upon cement strength development," *Powder Technology*, vol. 188, no. 3, pp. 272–276, 2009.

[11] C. Shi and R. L. Day, "A calorimetric study of early hydration of alkali-slag cement," *Cement and Concrete Research*, vol. 25, no. 6, pp. 1333–1346, 1995.

[12] P. Dinakar, K. P. Sethy, and U. C. Sahoo, "Design of self-compacting concrete with ground granulated blast furnace slag," *Materials and Design*, vol. 43, pp. 161–169, 2013.

[13] A. Bougara, C. Lynsdale, and N. B. Milestone, "Reactivity and performance of blastfurnace slags of differing origin," *Cement and Concrete Composites*, vol. 32, no. 4, pp. 319–324, 2010.

[14] M. Stefandiou and I. Papayianni, "Influence of nano-SiO_2 on the Portland cement pastes," *Composites Part B: Structure*, vol. 43, no. 6, pp. 2706–2710, 2012.

[15] P. Chindaprasirt, T. Sinsiri, W. Kroehong, and C. Jaturapitakkul, "Role of filler and pozzolanic reaction of biomass ashes on hydration phase and pore size distribution of blended cement paste," *Journal of Materials in Civil Engineering*, vol. 26, no. 9, article 04014057-10, 2014.

[16] K.-B. Park, H.-S. Lee, and X.-Y. Wang, "Prediction of time-dependent chloride diffusion coefficients for slag-blended concrete," *Advances in Materials Science and Engineering*, vol. 2017, Article ID 1901459, 10 pages, 2017.

[17] J. Tangpagasit, R. Cheerarot, C. Jaturapitakkul, and K. Kiattikomol, "Packing effect and pozzolanic reaction of fly ash in mortar," *Cement and Concrete Research*, vol. 35, no. 6, pp. 1145–1151, 2005.

[18] C. Jaturapitakkul, J. Tangpagasit, S. Songmue, and K. Kiattikomol, "Filler effect and pozzolanic reaction of ground palm oil fuel ash," *Construction and Building Materials*, vol. 25, no. 11, pp. 4287–4293, 2011.

[19] P. Norrarat, W. Tangchirapat, and C. Jaturapitakkul, "Evaluation of heat evolution of pastes containing high volume of ground river sand and ground granulated blast furnace slag," *Material Science (medziagotyra)*, vol. 23, no. 1, pp. 57–63, 2017.

[20] V. Kocaba, E. Gallucci, and K. L. Scrivener, "Methods for determination of degree of reaction of slag in blended cement pastes," *Cement and Concrete Research*, vol. 42, no. 3, pp. 511–525, 2012.

[21] C. Jaturapitakkul, J. Tangpagasit, S. Songmue, and K. Kiattikomol, "Filler effect of fine particle sand on the compressive strength of mortar," *International Journal of Minerals, Metallurgy, and Materials*, vol. 18, no. 2, pp. 240–246, 2011.

[22] ASTM C150, *Standard Specification for Portland Cement*, American Society for Testing and Materials, West Conshohocken, PA, USA, 2014.

[23] Q. Yang, S. Zhang, S. Huang, and Y. He, "Effect of ground quartz sand on properties of high-strength concrete in the steam-autoclaved curing," *Cement and Concrete Research*, vol. 30, no. 12, pp. 1993–1998, 2000.

[24] K. Kiattikomol, C. Jaturapitakkul, and J. Tangpagasit, "Effect of insoluble residue on properties of Portland cement," *Cement and Concrete Research*, vol. 30, no. 8, pp. 1209–1214, 2000.

[25] K. D. Weerdt, M. B. Hara, G. L. Saout, K. O. Kjellsen, H. Justnes, and B. Lothenbach, "Hydration mechanisms of ternary Portland cements containing limestone powder and fly ash," *Cement and Concrete Research*, vol. 41, no. 3, pp. 279–291, 2011.

[26] ASTM C230, *Standard Test Method for Flow Table for Use in Tests of Hydraulic Cement*, American Society for Testing and Materials, West Conshohocken, PA, USA, 2014.

[27] ASTM C109, *Standard Test Method for Compressive Strength of Hydraulic Cement Mortars (Using 2-in or [50 mm] Cube Specimens)*, American Society for Testing and Materials, West Conshohocken, PA, USA, 2014.

[28] T. Sinsiri, P. Chindaprasirt, and C. Jaturapitakkul, "Influence of fly ash fineness and shape on the porosity and permeability of blended cement pastes," *International Journal of Minerals, Metallurgy, and Materials*, vol. 17, no. 6, pp. 683–690, 2010.

[29] V. Sata, J. Tangpagasit, C. Jaturapitakkul, and P. Chindaprasirt, "Effect of W/B ratios on pozzolanic reaction of biomass ashes in Portland cement matrix," *Cement and Concrete Composites*, vol. 34, no. 1, pp. 94–100, 2012.

[30] E. Douglas, A. Elola, and V. M. Malhotra, "Characterization of ground granulated blast furnace slag and fly ashes and their hydration in Portland cement blends," *Cement Concrete and Aggregates*, vol. 12, no. 1, pp. 38–46, 1990.

[31] M. Ashraf, A. Naeem Khan, Q. Ali, J. Mirza, A. Goyal, and A. M. Anwar, "Physico-chemical, morphological and thermal analysis for the combined pozzolanic activities of minerals additives," *Construction and Building Materials*, vol. 23, no. 6, pp. 2207–2213, 2009.

[32] E. Güneyisi and M. Gesoğlu, "A study on durability properties of high-performance concretes incorporating high replacement levels of slag," *Materials and Structures*, vol. 41, no. 3, pp. 479–493, 2007.

[33] A. Elahi, P. A. M. Basheer, S. V. Nanukuttan, and Q. U. Z. Khan, "Mechanical and durability properties of high performance concretes containing supplementary cementitious materials," *Construction and Building Materials*, vol. 24, no. 3, pp. 292–299, 2010.

[34] M. Shariq, J. Prasad, and A. Masood, "Effect of GGBFS on time dependent compressive strength of concrete," *Construction and Building Materials*, vol. 24, no. 8, pp. 1469–1478, 2010.

[35] S. C. Pal, A. Mukherjee, and S. R. Pathak, "Investigation of hydraulic activity of ground granulated blast furnace slag in concrete," *Cement and Concrete Research*, vol. 33, no. 9, pp. 1481–1486, 2003.

[36] R. N. Swamy and A. Bouikni, "Some engineering properties of slag concretes as influenced by mix proportioning and curing," *ACI Materials Journal*, vol. 87, no. 3, pp. 210–220, 1990.

[37] J. Liu and D. Wang, "Application of ground granulate blast furnace slag-steel slag composite binder in a massive concrete structure under severe sulphate attack," *Advances in Materials Science and Engineering*, vol. 2017, Article ID 9493043, 9 pages, 2017.